*Polish Journal of Chemical Technology, 18, **4**, 41—46, 10.1515/pjct-2016-0069*

Model development of integrated CPOx reformer and SOFC stack system

Paulina Pianko-Oprych*, Seyed Mehdi Hosseini, Zdzislaw Jaworski

West Pomeranian University of Technology, Szczecin, Faculty of Chemical Technology and Engineering, Institute of Chemical Engineering and Environmental Protection Processes, al. Piastów 42, 71-065 Szczecin, Poland
**Corresponding author: e-mail: paulina.pianko@zut.edu.pl*

The main purpose of this study was to develop a mathematical model, in a steady state and dynamic mode, of a Catalytic Partial Oxidation (CPO_x) reformer – Solid Oxide Fuel Cell (SOFC) stack integrated system in order to assess the system performance. Mass balance equations were written for each component in the system together with energy equation and implemented into the MATLAB Simulink simulation tool. Temperature, gas concentrations, pressure and current density were computed in the steady-state mode and validated against experimental data. The calculated I–V curve matched well the experimental one. In the dynamic modelling, several different conditions including step changes in fuel flow rates, stack voltage as well as temperature values were applied to estimate the system response against the load variations. Results provide valuable insight into the operating conditions that have to be achieved to ensure efficient CPO_x performance for fuel processing for the SOFC stack applications.

Keywords: Catalytic Partial Oxidation (CPOx) reformer, Solid Oxide Fuel Cell (SOFC) stack, stead and dynamic mode, modelling.

INTRODUCTION

The Solid Oxide Fuel Cell (SOFC) is a promising alternative power source due to its advantageous properties such as high efficiency, low pollution and noise. One of the main advantages of the SOFC is the possibility of using carbon monoxide as fuel[1]. Thus, fuel flexibility allows to use not only hydrogen, but also reformed methane, LPG or LNG. In the case of the use of methane a partial oxidation on catalyst is applied for conversion of natural gas into a syngas[2]. Catalytic Partial Oxidation (CPO_x) of hydrocarbon fuels has been considered attractive due to rapid kinetics that permits volumetrically efficient syngas production without excessive amounts of fuel preheating and therefore it is a suitable technology to be used in compact SOFC based systems[3]. In addition, CPO_x provides superior start-up and transient responses, which are critical in small scale power applications. Therefore, in order to improve the design and optimization operability of various SOFC based systems a fundamental understanding of the CPO_x reformers with higher hydrocarbons is a basis. One of the first Matlab Simulink simulations was applied for the system net powers between 1 and 5 kW. Simulation results indicated that a peak electrical efficiency of 30% with respect to the LHV of diesel was realistic[4]. The development of an advanced, planar, compact SOFC stack with a nominal electrical power of 1.5 kW_{el} and CPO_x based system was also presented within the FC-DISTRIBCT micro-CHP system[5]. Reformer efficiencies up to approximately 88% were reached for operation with natural gas in a wide range of air/fuel ratio from 0.17 to 0.33 and different initial preheating temperatures from 20°C to 450°C. It was noticed that an air to fuel ratio of 0.31 used in the CPO_x for full load operation of the micro-CHP system was chosen as a compromise between high performance and safety relevant to overheating conditions. Kupilik and Vincent[6] presented the use of a model predictive control algorithm on a solid oxide fuel cell system including CPO_x reformer, blowers, heat exchanger, tail gas burner and stack. The algorithm was designed to control the flow rates of fuel and air delivered to the stack in order to ensure both the required current and appropriate fuel reformer operational conditions as well as to prevent coking. The CPO_x reactor was considered as a continuous stirred tank reactor with surface chemistry. A CSTR was used to capture temperature and composition of the reformate. However, the authors[6] mentioned that a plug flow model would be more accurate. The developed model was validated against an experimental CPO_x reformer at the Colorado Fuel Cell Center. It was shown that the controller was capable of staying within desired operating temperatures and ensuring the reformer produces a fuel, which was not prone to carbon formation. Encouraged by the previous SOFC system simulation results, we decided to develop a user friendly and versatile tool aimed at controlling and optimization of the integrated CPO_x reformer and SOFC stack system by taking into account thermodynamic and electrochemical aspects for describing the single cell behaviour as well as system process parameters including gas feeding circuits. It was expected that the developed approach should be helpful in the BoP components design within the 7FP project with acronym STAGE-SOFC.

MODELLING APPROACH

A proposed modelling approach was implemented into a flexible Matlab SIMULINK environment. The model of the system was based upon a set of fundamental equations accounting for fluid dynamics, thermal dynamics and kinetic behaviour of feed streams including two main system components: CPO_x reformer and SOFC stack.

The methane fuel was fed to the CPO_x reformer for conversion to syngas. The hydrogen and carbon monoxide from the reformer were fed to the SOFC stack to generate electric power and heat.

For the CPO_x reformer, a mathematical model was based on a similar approach as used by Pukrushpan et al.[7], where four chemical reactions were considered. The first two reactions of partial oxidation (POX) and total oxidation (TOX) were discussed in details in paper[8], while the other two reactions of hydrogen oxidation (HOX) and carbon monoxide oxidation (COX) were presented

Table 1. CPO_x reformer reactions

Reaction name	Reaction	Reaction enthalpy
POX	$CH_4 + 0.5O_2 \rightarrow CO + 2H_2$	$\Delta H^0_{POX} = -36$ kJ/mole
TOX	$CH_4 + 2O_2 \rightarrow CO_2 + 2H_2O$	$\Delta H^0_{TOX} = -802.6$ kJ/mole
HOX	$2H_2 + O_2 \rightarrow 2H_2O$	$\Delta H^0_{HOX} = -483.6$ kJ/mole
COX	$2CO + O_2 \rightarrow 2CO_2$	$\Delta H^0_{COX} = -566$ kJ/mole

in paper[9]. A list of reactions used in the CPO_x reformer model is shown in Table 1.

The amount of hydrogen produced in the CPO_x reformer depended on the catalyst bed material, temperature and oxygen to carbon ratio (λ_{O_2C}). The lambda number, λ_{O_2C} , represents the molar ratio of the oxygen to carbon entering the CPO_x reformer and it was defined as follows:

$$\lambda_{O_2C} = \frac{N_{O_2,in}}{N_{CH_4,in}} \tag{1}$$

where: $N_{O_2,\,in}$ and $N_{CH_4,\,in}$ were molar flow rates of the oxygen and methane entering the CPO_x reformer. The following assumptions were employed to simplify the study of the CPO_x reformer:

– gas compositions and temperature of the flow entering the reformer were constant;

– ideal gas laws were applied to flows;

– gas mixtures were treated as perfect mixtures;

– influence of temperature variations on the partial pressure dynamics was assumed negligible;

– a volume of CPO_x reformer was relatively small and thus it was ignored;

– CPO_x reactions had rapid kinetics and reached equilibrium condition before the flow exit the reactor control volume.

Since the gas volume in the CPO_x catalyst bed was relatively small, the gas inertia was ignored. The only dynamic quantity considered in the CPO_x was the catalyst temperature, $C_{P_{CPO_x}}$. The temperature dynamics was modelled using an energy balance equation (2)[7]:

$$m_{CPO_x,bed} C_{p_{CPO_x,bed}} \frac{dT_{CPO_x}}{dt} = \left(T_{in,CPO_x} - T_{ref}\right)\sum_{i=1}^{n} C_{p,i} M_i W_i - \\ -\left(T_{CPO_x} - T_{ref}\right)\sum_{j=1}^{n} C_{p,j} M_j W_j + \left[\text{heat of reactions}\right] \tag{2}$$

where:

$M_{CPO_x,bed}$ and $C_{p_{CPO_x},bed}$ are mass and specific heat capacity of the catalyst bed, respectively. Index *i* represents four species in the inlet flow and *j* represents the species at the outlet flow. T_{ref} and $T_{in,\,CPO_x}$ are the reference temperature (298 K) and inflow temperature. $C_{p,i}$and $C_{p,j}$ are the specific heat of the reactants. M_i and W_i are the molar mass of the reactants and their molar flow rate, respectively.

The three key variables that define the calculation of CPO_x reaction rates were: α, S, and β. Their definitions are as follows[7]:

$$\alpha = \frac{\text{rate of } CH_4 \text{ reacting}}{\text{rate of } CH_4 \text{ entering}} \tag{3}$$

$$\beta = \frac{\text{rate of } O_2 \text{ reacts with } H_2}{\text{rate of } O_2 \text{ reacts with } H_2 \text{ and CO}} \tag{4}$$

$$S = \frac{\text{rate of } CH_4 \text{ reacting in POX}}{\text{total rate of } CH_4 \text{ reacting}} \tag{5}$$

For values of S close to one, the POX reaction rate was higher than the TOX reaction rate and thus more hydrogen was generated. Since there were two moles of H_2 produced per one mole of CO produced in POX reaction, more O_2 reacted with H_2 than with CO and, thus, the ratio β was kept constant at β = 0.66[8]. For lambda numbers smaller than 0.5, the amount of oxygen was not sufficient to oxidize methane flow inside the reformer and the amount of the hydrogen released in the reactions was limited by oxygen. To avoid fuel waste, the lambda number was kept higher than 0.5 in normal operation condition. In order to avoid an ignition inside the anode, there should not be any oxygen inside CPO_x outflow. Furthermore, a high value of lambda number indicated high reaction rate for TOX. Since more heat was released from TOX reaction, the temperature of the reformer increased and it could permanently damage the catalyst bed[6, 8]. The set of equations to calculate the molar flow rates of each reactants outflowing the CPO_x reformer was as follow:

$$N_{H_2} = \left[2S\alpha - 2\beta\left(\lambda_{O_2C} - \lambda_\chi \alpha\right)\text{sign}(S)\right] N_{CH_4,in} \tag{6}$$

$$N_{CO} = \left[S\alpha - 2(1-\beta)\left(\lambda_{O_2C} - \lambda_\chi \alpha\right)\text{sign}(S)\right] N_{CH_4,in} \tag{7}$$

$$N_{CO_2} = \left[(1-S)\alpha - 2(1-\beta)\left(\lambda_{O_2C} - \lambda_\chi \alpha\right)\text{sign}(S)\right] N_{CH_4,in} \tag{8}$$

$$N_{H_2O} = \left[2(1-S)\alpha - 2\beta\left(\lambda_{O_2C} - \lambda_\chi \text{sign}(S)\right)\right] N_{CH_4,in} + N_{H_2O_{in}} \tag{9}$$

$$N_{CH_4} = (1-\alpha) N_{CH_4,in} \tag{10}$$

$$N_{O_2} = \left[N_{O_2,in} - \lambda_\chi \alpha N_{CH_4,in}\right]\text{sign}(S) \tag{11}$$

$$N_{N_2} = N_{N_2,in} \tag{12}$$

$$\lambda_\chi = 2 - 1.5S \tag{13}$$

where: N_{H2Oin} and $N_{O_2,in}$ are respectively the molar flow rates of the water steam and nitrogen entering the CPO_x reformer. The heat released from the reaction depended on the extent of reaction taking place in the following way:

$$\left[\text{heat of reactions}\right] = \alpha N_{CH_4,in}\left(S \cdot \Delta H^0_{POX}\right) + \left((1-S)\cdot \Delta H^0_{TOX}\right) + \\ + N_{O_2rCOH_2}\left(\beta \cdot (-\Delta H^0_{HOX}) + (1-\beta)\cdot(-\Delta H^0_{COX})\right) \tag{14}$$

Table 2. Reactions considered in the MATLAB Simulink stack model[10]

Location	Reaction	Equation
Fuel channel	SR	$CH_4 + H_2O \rightarrow 3H_2 + CO$
	WGS	$CO + H_2O \leftrightarrow H_2 + CO_2$
Anode	Ox	$H_2 + O^{2-} \rightarrow H_2O + 2e^-$
Cathode	Red	$0.5O_2 + 2e^- \rightarrow O^{2-}$

$$N_{O_2rCOH_2} = \left(\lambda_{O_2C} - \lambda_\chi \text{sign}(S)\right) \tag{15}$$

The model of the SOFC stack was built based upon H_2 and CO reactions with water steam shown in Table 2.

In order to study transient behaviour of the SOFC stack at various operation conditions, the physical parameters of the stack were considered by neglecting three-

dimensional distributions of variables, such as current density, temperature, molar fraction of the reactants and pressures, along the flow channel. These variables were assumed homogeneous in the fuel cell and thus the dynamic governing equations were derived by applying the electrochemical, energy and mass balance equations.

Electrochemical sub-model

The operation voltage of the fuel cell, U_C, was calculated from Equation (16):

$$U_C = U_{OCV} - U_O \tag{16}$$

The open circuit voltage, U_{OCV}, was defined in Eq. (17):

$$U_{OCV} = N\left[\Delta E_0 + \frac{RT_{St}}{2Fp}\ln\frac{p_{H_2O}p_2^{0.5}}{{}_{H_2O}}\right] \tag{17}$$

where:

is the standard cell potential, p_{H_2} p_{O_2} and p_{H_2O} are the partial pressures of hydrogen, oxygen and steam, respectively, R and F are the universal gas constant and Faraday number, while N is the number of the cells in the stack and T_{St} is the stack temperature[11, 12].

The standard fuel cell potential was estimated from Equation (18):

$$\Delta E_0 = 1.2586 - 0.000252T_{St} \tag{18}$$

while the fuel cell voltage losses, U_0, was calculated from Equation (19):

$$U_0 = iASR = i\left(A\exp\left[B\left(\frac{1}{T_{St}} - \frac{1}{T_{ref}}\right)\right] + C\right) \tag{19}$$

where: *i* is the stack drawn current. An influence of pressure and reactant ratio was neglected. The constants A, B, C and T_{ref} have to be determined for each cell type. These constants can be estimated by fitting the ASR function to experimental data or by calculation from the fuel cell specific parameters.

Mass balance sub-model

In the sub-model, dynamic equations were derived to calculate species partial pressure of the bulk flows in the fuel and air channels. For each reactant, its mass balance equation inside the stack channel was written as:

$$\frac{dP_i}{dtV} = \frac{RT_{St}}{}\left(\dot{n}_i^{in} + \dot{n}_i^{react} - \dot{n}_i^{out}\right) \tag{20}$$

where: P_i is partial pressure of i-th reactant, V is the volume of the anode or cathode. $\dot{n}_i^{in}$ is molar flow rate of species entering the stack, $\dot{n}_i^{react}$ is molar reaction rate of each reactant inside the channels and $\dot{n}_i^{out}$ is the molar flow rate of the outflows from the anode and cathode. According to the Faraday's law, the rates of oxidation and redox reactions were related to the current density, thus:

$$R_r = \frac{Ni}{2F} \tag{21}$$

The rate of an internal steam reforming (SR) reaction inside the SOFC stack was applied according to the approach developed by[10]:

$$R_{SR} = k_{SR}p_{CH_4}\exp\left(-\frac{E_{SR}}{RT_{St}}\right) \tag{22}$$

where:

k_{SR} = 0.04274 (mol/cm^{2}Pa) and E_{SR} = 82 (kJ/mol). The Water Gas Shift (WGS) reaction is usually considered to be very fast at temperatures higher than 600 K and in this case was assumed that it reaches its equilibrium condition[13]:

$$R_{WGS} = k_{WGS}p_{CO}\left(1 - \frac{p_{CO_2}p_{H_2}}{p_{CO}p_{H_2O}K_{eq,WGS}}\right) \tag{23}$$

The partial pressures used in the Eq. (23) were the average of the inflow partial pressures and the outflow partial pressure. A constant value of the reaction rate k_{WGS} = 0.0000125 (mol/cm^{2}Pa) was applied. $K_{eq,WGS}$ was calculated from Equation (24)[13]:

$$K_{eq,WGS} = \exp\left(\frac{4276}{T_{St}} - 3.961\right) \tag{24}$$

The following Equations (25–29) were used for the reactions rates of the reactants inside the anode:

$$\dot{n}_{CH_4}^{react} = -R_{SR} \tag{25}$$

$$\dot{n}_{H_2O}^{react} = -R_{SR} - R_{WGS} + R_r \tag{26}$$

$$\dot{n}_{H_2}^{react} = 3R_{SR} + R_{WGS} - R_r \tag{27}$$

$$\dot{n}_{CO}^{react} = R_{SR} - R_{WGS} \tag{28}$$

$$\dot{n}_{CO_2}^{react} = R_{WGS} \tag{29}$$

while the reaction rate of the oxygen inside the cathode channel was estimated from Equation (30):

$$\dot{n}_C^{react} = -0.5R_r \tag{30}$$

where:

$\dot{n}_i^{in}$ was determined by the fuel and air inlet condition, $\dot{n}_i^{out}$ was defined by the following relation of the fuel and air flow stability (Eq. (31)):

$$\dot{n}_i^{out} = \alpha(P_0)y_i \tag{31}$$

where: P_0 is the total pressure of the downstream flow and y_i is the molar fraction of the reactant in the flow, α is the orifice constant of the fuel channel.

Energy balance sub-model

The temperature variation along the flow direction was assumed constant, and thus, the dynamics of the electrode temperature, T_{St}, can be expressed as a function of diffusive, convective and reactive heat transfer terms. Energy balance equation for the adiabatic fuel cell boundary was described based on Equations (32–33):

$$m_eC_{pe}\frac{dT_{St}}{dt} = \sum n_i^{in}\int_{T_{ref}}^{T_{in}}C_{p,i}(T)dT - \sum n_i^{out}\int_{T_{ref}}^{T_{St}}C_{p,i}(T)dT - \\ -\sum R_j\Delta\hat{H}_j - \dot{W} \tag{32}$$

$$\dot{W} = V_s \cdot I \tag{33}$$

where: m_e and C_{pe} are the total mass and average specific heat of fuel cell materials excluding gases, (specifically, electrode and interconnector) respectively. R_j and $\Delta\hat{H}_j$ are the reaction rates and the specific heat of reactions, $Cp_{,i}$ is the specific heat of the reactants entering the anode or cathode, $\dot{n}_i^{in}$ and $\dot{n}_i^{out}$ are the molar flow rate of the reactants entering and exiting the SOFC stack.

In this work, the following assumptions were also employed to simplify the dynamic study of the SOFC:

– gases were assumed to obey ideal gas laws and gas mixtures were treated as perfect mixtures;

– electrochemical reactions occurred at the electrode–electrolyte boundaries;

– density and heat capacity of the solid components were temperature independent;

– parameters for individual cells can be lumped together to represent a fuel cell stack;

– adiabatic boundaries for the cell were used.

SIMULATIONS

Figure 1 shows the simulation model developed in the Matlab SIMULINK software. The dynamic model consists of a set of nonlinear Ordinary Differential Equations (ODE). The model incorporates two main components: CPO_x reformer subsystem and SOFC stack subsystem. The inputs of the system: for the CPO_x reformer are natural gas flow rate, and lambda number, while for the SOFC stack subsystem they are as follows: cathode inlet air flow rate, cathode temperature and stack drawn current as shown in Figure 1. The model parameters are presented in Table 3.

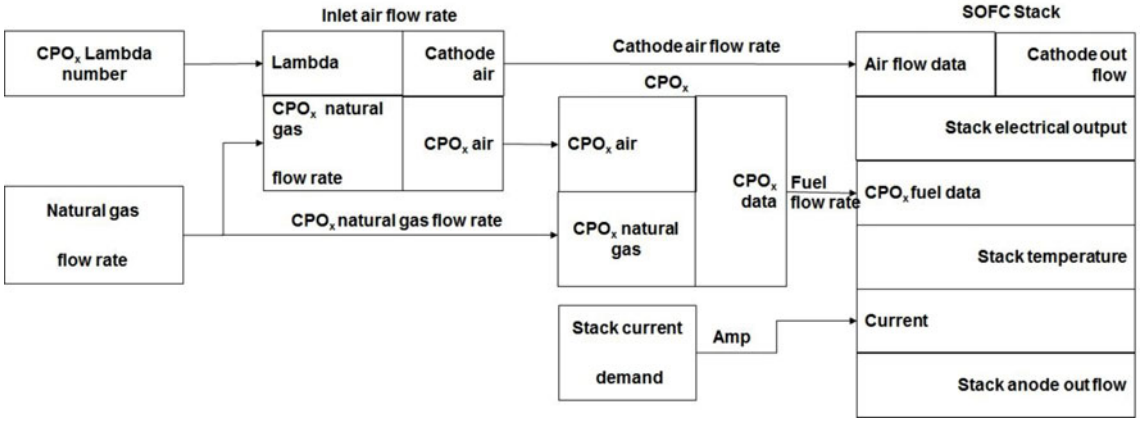

Figure 1. Integrated CPO_x reformer and SOFC stack system simulation model

Table 3. Model parameters of the system

Parameter	Value	Unit
Number of cells	16	–
Cell active area	8.079	cm^2
Electrolyte thickness	1	μm
Electrolyte density	5800	kg/m^3
Electrolyte specific heat capacity	600	J/kg · K
Fuel and air channel volume	21.3853	mm^3
Interconnector thickness	0.5	mm
Interconnector density	7800	kg/m^3
Interconnector specific heat capacity	660	J/kg · K
Bulk density of CPOx reformer	470	kg/m^3
CPOx bed specific heat capacity	280	J/kg · K

The developed model is suitable for simulating fuel cell behaviour under various operating conditions and thus it can be also used to evaluate and select system components for developing hybrid power systems.

RESULTS

To validate the accuracy of the integrated CPO_x reformer and SOFC stack prediction, the calculated V-I curve was compared with a set of experimental data as shown in Figure 2 and a good agreement of the two was observed.

Figure 3a presents the output voltage of SOFC at different inlet gas temperatures. The cell voltage was higher at lower temperatures and at lower current densities, while the voltage at higher temperatures was higher in the high current density region. The cell power density curves are presented in Figure 3b. At low current densities the stack power density was similar for different temperatures. By increasing the operating temperature of the SOFC stack, the optimum current density of the stack increases as well. On the other hand, lifetime of the SOFC stack decreases at high temperatures.

To analyse the dynamic response of the SOFC stack, step changes in the stack power demand were assumed as it is shown in Figure 4. In the first approach, the CPO_x lambda number was equal to 0.61, while the natural gas flow rate to the CPO_x was 0.000337 [mol/s] at 20°C, with the cathode air flow of 0.01096 [mol/s] at 650°C. The stack drawn current signal was changing between 9.675 A to 6.525 A.

The effect of the current change on the SOFC stack dynamics is presented in Figure 5a. It can be noticed

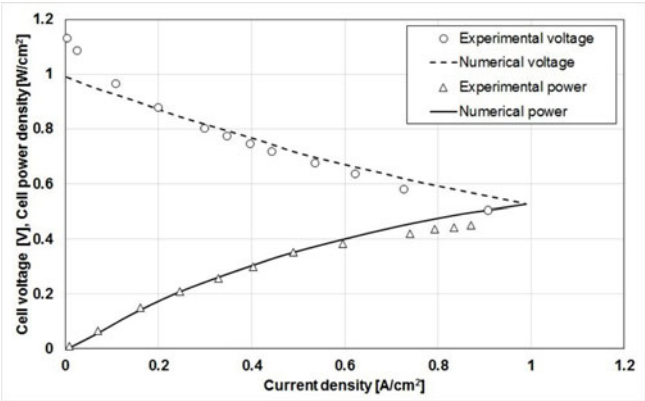

Figure 2. V-I curve for SOFC

that a 32.5% decrease in the stack drawn current leads to 2.73% increase in the fuel cell and stack terminal voltages as well as to 4.3% decrease in the stack temperature. A decrease in the stack current leads to lower oxidation rate inside the stack and, as a consequence, to lower heat production.

In the second approach, the impact of the CPO_x reformer operating lambda number on the system performance was studied (Fig. 6). In this case the stack drawn current was assumed to be equal 8.5 A, while the remaining parameters were similar as in the first approach.

The temperature of the CPO_x reformer during the simulations is presented in Fig. 7a along with the outflow rate (Fig. 7b). When increasing the lambda number, the amount of excessive oxygen in the CPO_x reformer inlet flow rate increases and this leads to higher total

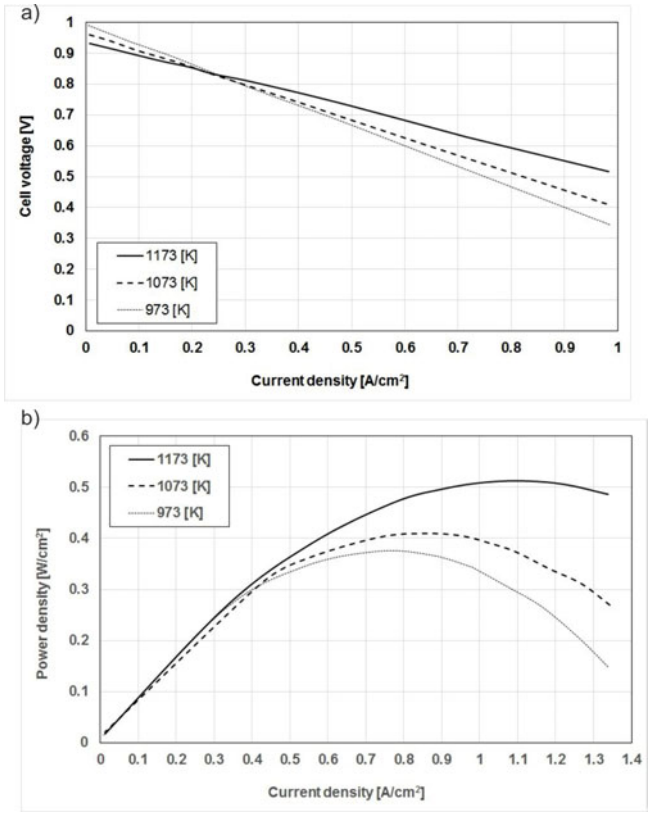

Figure 3. Temperature dependence of the V-I characteristics for SOFC (a) and power density vs. current density curves for the SOFC at different operating temperatures (b)

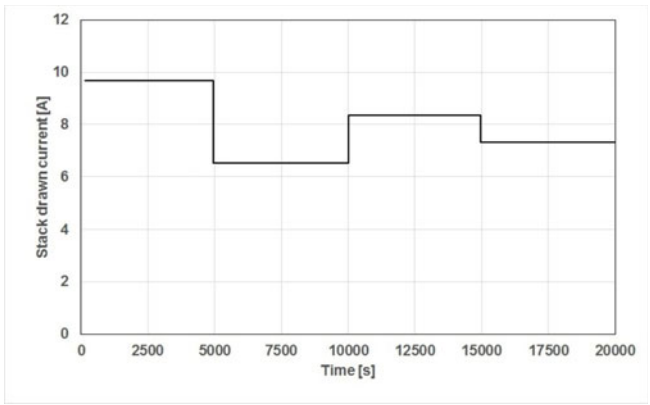

Figure 4. Stack drawn current

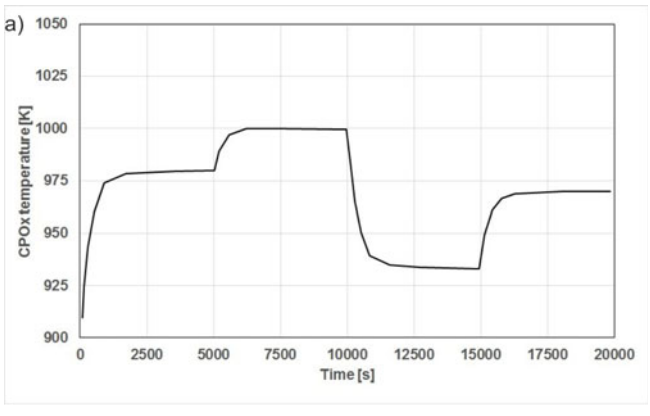

Figure 7. CPOx reformer temperature (a) and outflow rate (b)

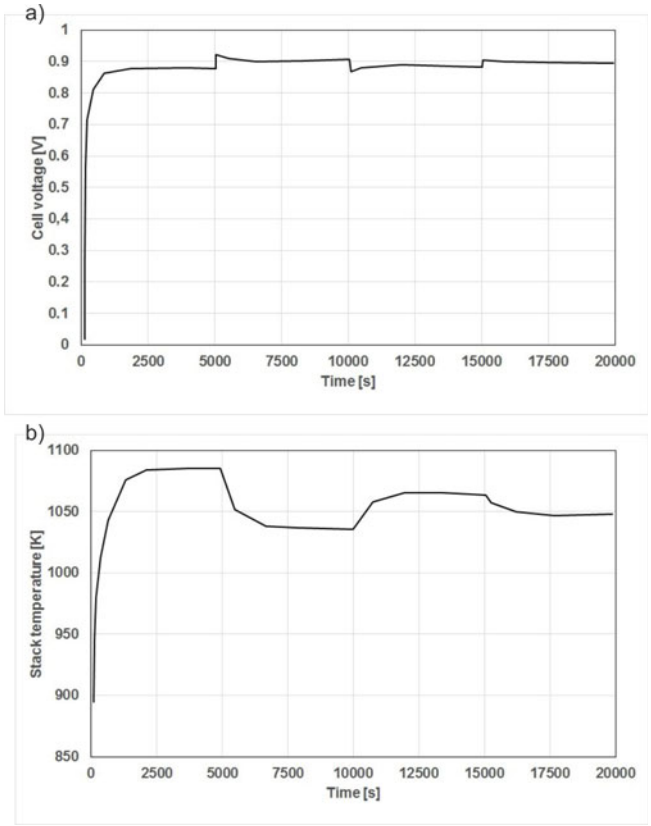

Figure 5. Dynamic response of the SOFC stack for different stack drawn current values: (a) cell voltage [V], (b) stack temperature [K]

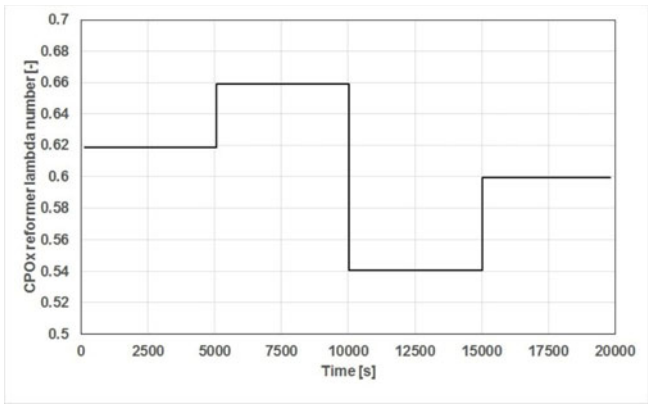

Figure 6. Variation of the CPO_x reformer operating lambda number

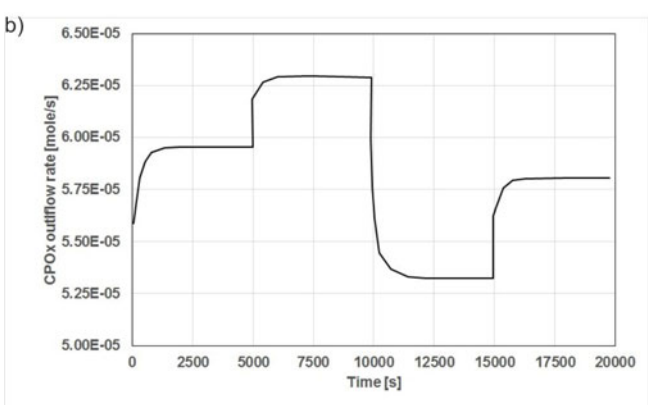

(TOX) and partial oxidation (POX) reaction rates inside the reformer. Therefore, the temperature of the CPO_x reformer increases due to generation of higher amount of heat during reactions. In each case, growth of the CPO_x reformer operating lambda number caused the cell voltage and stack power decrease (Fig. 8a). However, temperatures obtained in the simulations for the CPO_x reformer were slightly too high and thus further studies and modification of the CPO_x reformer model are needed.

The Open Circuit Voltage (OCV) of the SOFC stack is a function of stack temperature. A decrease in the

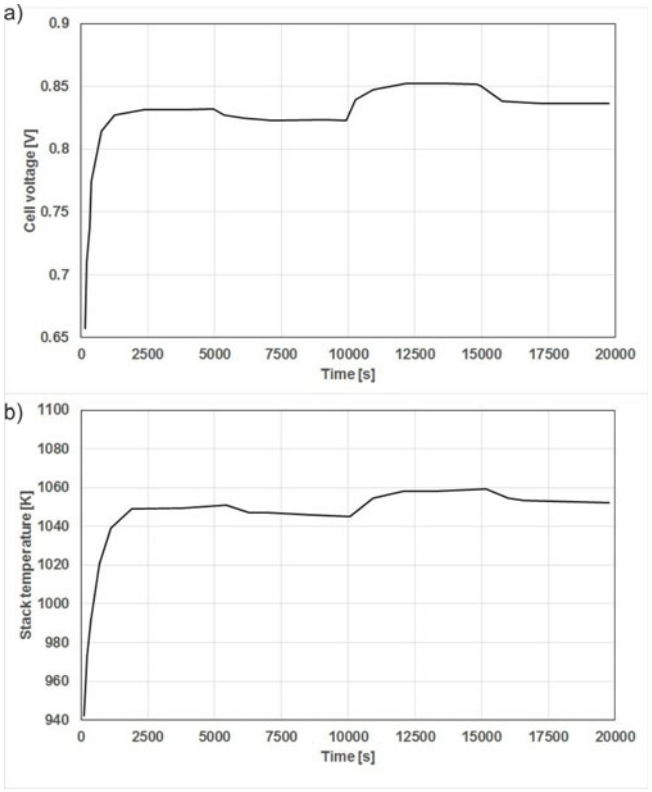

Figure 8. Dynamic response of the SOFC stack for different CPO_x reformer operating lambda number values: (a) cell voltage [V], (b) stack temperature [K]

stack temperature causes the OCV drop as it can be seen in Fig. 8b.

CONCLUSIONS

The main aim of the presented work was to construct a valid and modular model of the integrated CPO_x reformer and SOFC stack system that could be useful in various applications such as designing and developing system components in order to improve the system configuration. At first, a steady-state SOFC based system model was defined, ran and compared with the experimental data. The numerical results of the polarization curve showed a good agreement with the experimental ones. In the second step, dynamics analysis for the most typical operating conditions was performed. The Simulink results were valid in a large range of the CPO_x reformer – SOFC based system operations under unsteady state conditions. It should be underlined that the modelling was straightforward and not demanding in terms of computing time. Thus, it can be concluded that the BoP results presented in this paper can be very useful in optimizing system parameters.

ACKNOWLEDGMENTS

The research programme leading to these results received funding from the European Union's Seventh Framework Programme (FP7/2007–2013) for the Fuel Cells and Hydrogen Joint Undertaking (FCH JU) under grant agreement n° [621213]. Information contained in the paper reflects only view of the authors. The FCH JU and the Union are not liable for any use that may be made of the information contained therein. The work was also financed from the Polish research funds awarded for the project No. 3126/7.PR/2014/2 of international cooperation within STAGE-SOFCI in years 2014–2017.

LITERATURE CITED

1. Bae, J., Lim, S., Jee, H., Kim, J.H., Yoo, Y.S. & Lee, T. (2007). Small stack performance of intermediate temperature operating solid oxide fuel cells using stainless steel interconnects and anode supported single cell. J. Power Sour. 172, 100–107. DOI: 10.1016/j.jpowsour.2007.01.093.

2. Tavazzi, I., Beretta, A., Groppi, G., Forzatti, P., Bao, X. & Xu, Y. (2004). An investigation of methane partial oxidation kinetics over Rh supported catalysts, Studies Surface Science Catalysis – Natural Gas Conversion VII, 147, Elsevier, Amsterdam, 163–168. DOI: 10.1016/S0167-2991(04)80045-4.

3. Seyed-Reihani, S.A. & Jackson, G.S. (2010). Catalytic partial oxidation of n-butane over Rh catalysts for solid oxide fuel cell applications. Catal. Today, 155, 75–83. DOI: 10.1016/j.cattod.2009.03.032.

4. Lawrence, J. & Boltze, M. (2006). Auxiliary power unit based on a solid oxide fuel cell and fueled with diesel J. Power Sour. 154, 479–488. DOI: 10.1016/j.jpowsour.2005.10.036.

5. Frenzel, I., Loukou, A., Trimis, D., Schroeter, F., Mir, L., Marin, R., Egilegor, B., Manzanedo, J., Raju, G., de Bruijne, M., Wesseling, R., Fernades, S., Pereira, J.M.Ch., Vourliotakis, G., Founti, M. & Posdziech, O. (2012). Development of an SOFC based micro-CHP system in the framework of the European project FC-DISTRICT. Energy Proc. 28, 170–181. DOI: 10.1016/j.egypro.2012.08.051.

6. Kupilik, M. & Vincent, T.L. (2013). Control of a solid oxide fuel cell system with sensitivity to carbon formation. J. Power Sour. 222, 267–276. DOI: 10.1016/j.jpowsour.2012.08.083.

7. Pukrushpan, J., Stefanopoulou, A., Varigonda, S., Eborn, J. & Haugstetter, C. (2006). Control oriented model of fuel processor for hydrogen generation in fuel cell applications, Control Engine. Pract. 14(3), 277–293. DOI: 10.1016/j.conengprac.2005.04.014.

8. Zhu, J., Zhang, D. & King, K.D. (2001). Reforming of CH_4 by partial oxidation: thermodynamic and kinetic analyses. Fuel 80(7), 899–905. DOI: S0016-2361(00)00165-4.

9. Larentis, A.L., de Resende, N.S., Salim, V.M.M. & Pinto, J.C. (2001). Modeling and optimization of the combined carbon dioxide reforming and partial oxidation of natural gas. Appl. Catal. 215(1–2), 211–224. DOI: S0926-860X(01)00533-6.

10, Xi, H., Sun, J. & Tsourapas, V. (2007). A control oriented low order dynamic model for planar SOFC using minimum Gibbs free energy method. J. Power Sour. 165(1), 253–266. DOI: 10.1016/j.jpowsour.2006.12.009.

11. Singhal, S. & Kendall, K. (2004). High temperature Solid Oxide Fuel Cells: Fundamentals, Des. Applicat. Elsev. Sci. ISBN: 978-1-85617-387-2.

12. Larminie, J. & Dicks, A. (2003). Fuel Cell Systems Explained, 2nd Edition, Wiley. ISBN: 0-470-84857-X.

13. Aguiar, P., Adjiman, C.S. & Brandon, N.P. (2006). Anode supported intermediate temperature direct internal reforming solid oxide fuel cell. I: Model based steady-state performance. J. Power Sour. 138(1–2), 120–136. DOI: 10.1016/j.jpowsour.2004.06.040.